Eur. Phys. J. D (2022)76:128
https://doi.org/10.1140/epjd/s10053-022-00459-7

THE EUROPEAN PHYSICAL JOURNAL D

Regular Article – Molecular Physics and Chemical Physics

Comparing pulsed and continuous laser-induced acoustic desorption (LIAD) as sources for intact biomolecules

Siwen Wang, Grite L. Abma, Peter Krüger, Andre van Roij, Michiel Balster, Niek Janssen, and Daniel A. Horke[a]

Institute for Molecules and Materials, Radboud University, Heijendaalseweg 135, 6525 AJ Nijmegen, The Netherlands

Received 8 June 2022 / Accepted 9 July 2022

Abstract. A major obstacle to the gas-phase study of larger (bio)molecular systems is the vaporisation step, that is, the introduction of intact sample molecules into the gas-phase. A promising approach is the use of laser-induced acoustic desorption (LIAD) sources, which have been demonstrated using both nanosecond pulsed and continuous desorption lasers. We directly compare here both approaches for the first time under otherwise identical conditions using adenine as a prototypical biological molecule, and study the produced molecular plumes using femtosecond multiphoton ionisation. We observe different desorption mechanisms at play for the two different desorption laser sources; however, we find no evidence in either case that the desorption process leads to fragmentation of the target molecule unless excessive desorption energy is applied. This makes LIAD a powerful approach for techniques that require high density and high purity samples in the gas-phase, such as ultrafast dynamics studies or diffraction experiments.

1 Introduction

Over the last decades supersonic molecular beams have been the workhorse of gas-phase spectroscopy studies and are routinely used from x-ray to microwave spectral ranges. However, when it comes to studying larger (bio)molecular systems, a major limitation is still the introduction of intact target molecules into the expanding gas mixture, which is typically done through heating of a sample reservoir. This precludes thermally labile molecules from study, and has led to the development of alternative approaches to introduce labile species into an expanding gas mixture. The most prominent of these is laser desorption, in which target molecules are mixed with a matrix material (typically graphite) and then desorbed from the matrix by an IR laser pulse directly in front of the supersonic expansion nozzle [1–3]. This approach has been very successful in introducing large systems, including polypeptides and clusters thereof, into the gas-phase [4–6]. However, it has also been shown that it can lead to significant fragmentation of the target system, and hence might not produce a clean molecular beam [7]. This makes it difficult to implement these molecular sources into experiments that rely on a pure molecular sample.

An alternative approach to vaporise thermally labile systems, which was also introduced several decades ago but has received relatively little attention, is laser-induced acoustic desorption (LIAD) [8]. In this approach the target molecule is deposited on a thin metal substrate, which is irradiated by a desorption laser from the backside, thus avoiding any direct contact between the laser and the target system. The LIAD approach has now been adopted by a number of groups, and demonstrated with both continuous-wave [9,10] and nanosecond pulsed lasers used for desorption [11–15]. However, open questions remain about whether or not the LIAD process introduces fragmentation of target systems in the produced molecular plume [16]. Furthermore, no direct comparison between the nanosecond pulsed desorption (ns-LIAD) and continuous desorption (cw-LIAD) has been presented. Whilst for many applications desorption-induced fragmentation is not relevant, such as resonance-based spectroscopy, it is crucial for the use of LIAD in experiments that require pure molecular targets, such as ultrafast dynamics studies, strong-field experiments or diffraction-based imaging approaches. Moreover, the nature of the desorption mechanism behind LIAD still remains actively discussed [16–18], and likely depends not only on the desorption laser source (continuous or nanosecond pulsed), but also on further experimental parameters such as the thickness of the sample layer or the material of the metal substrate. Previously employed substrate materials include stainless steel [10,19], tantalum [9,20] and titanium [14,21], typically chosen for their high melting point and low thermal conductivity.

In this contribution, we show that LIAD using nanosecond or continuous desorption lasers, under the right experimental conditions, does not lead to any significant fragmentation. We demonstrate this for the target system adenine, which is brought into the gas-

[a] e-mail: d.horke@science.ru.nl (corresponding author)

Published online: 23 July 2022

phase using ns-LIAD or cw-LIAD under otherwise identical experimental conditions. The produced molecular plume is analysed using femtosecond multiphoton ionisation. For both pulsed and continuous desorption regimes we observe that increasing the desorption laser intensity leads to a significant increase in the observed signal, but does not influence the molecular fragmentation over a wide range of desorption energies. Only at very high energies was an increase in fragmentation observed, likely due to excessive heating of the sample. We furthermore observe a significant difference in the desorption laser dependence of the ion signal for ns-LIAD and cw-LIAD, pointing to different desorption mechanisms at play in the two regimes. We demonstrate that the LIAD approach is hence a viable molecular source for gas-phase experiments that require pure molecular targets, and offers a route to producing high-density samples of intact large (bio)-molecules that is widely applicable to gas-phase spectroscopy studies.

2 Methods

A detailed description of the experimental setup, containing a taper-device for constant sample replenishment, has been given previously [16]. For the current experiments sample was deposited onto a 10 μm thick titanium foil (Baoji Energy Titanium Co.). Titanium was chosen for its high melting point and low thermal conductivity, its relatively constant reflectivity over the wavelength range of the employed desorption lasers [22], and its proven effectiveness in previous LIAD experiments [14]. For ns-LIAD experiments this was irradiated from the backside by the third harmonic (355 nm) of a nanosecond Nd:YAG laser (Innolas Spitlight 1200, ∼8 ns pulse duration) operating at ∼50 Hz. Desorption pulses were attenuated to 0.2–1.6 mJ and focused onto the foil using a $f = 500$ mm lens, leading to an irradiated area on the foil of approximately 0.35 mm^2. For cw-LIAD experiments, desorption was driven by a fibre-coupled laser diode operating at 445 nm (Wavespectrum Laser). This was guided into the chamber via a multimode optical fibre (100 μm diameter, 0.22 NA). The fibre output inside vacuum was placed approximately 5 mm before the foil surface without further collimation. The irradiated area in the horizontal direction was controlled using two knife edges, which created an effective irradiated area on the foil of approximately 3×0.2 mm. The total power incident on the foil was controlled via the laser diode current, and limited to 20–100 mW.

Desorbed molecules were ionised by a femtosecond laser system comprising a titanium–sapphire oscillator and regenerative amplifier (Spectra Physics *Spitfire Ace*) with a fundamental output at 800 nm, operating at 3 kHz repetition rate with typical pulse durations of 100 fs. For ns-LIAD experiments the repetition rate was reduced to match that of the YAG laser. Femtosecond laser pulses were kept at 220 μJ throughout, and focused into the interaction region of a Wiley–McLaren type linear time-of-flight mass spectrometer using a $f = 500$ mm lens. Ions are detected by a 18 mm diameter microchannel-plate detector, where single ions hits are recorded and time-stamped using a combination of constant fraction discriminator (Surface Concept GmbH) and time-to-digital converter (cronologic GmbH).

Adenine sample was purchased from Sigma-Aldrich and used without further purification. The sample was dissolved in water to make a 15 mM solution, which was sprayed onto the titanium foil using a simple commercial airbrush spray-gun (nozzle size 0.2 mm, backing pressure 1.0 bar). After application of the sample the water was left to evaporate before transferring the foil to the taper device in the vacuum chamber. During measurements the foil is replenished at a speed of 125 μm/s.

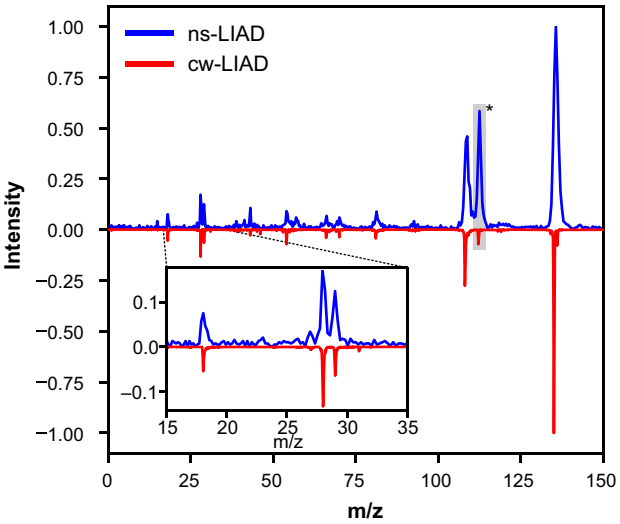

Fig. 1 Normalised mass spectra of adenine following desorption by ns-LIAD (blue) or cw-LIAD (red), and multiphoton ionisation by 800 nm femtosecond pulses ($\sim 1.4 \times 10^{13}$ W/cm^2). The shaded peak marked with an asterisk is due to a background contamination in the vacuum chamber

3 Results and discussion

Typical mass spectra of adenine following desorption using ns-LIAD or cw-LIAD and multiphoton ionisation using 800 nm femtosecond pulses are shown in Fig. 1. These were collected under identical experimental conditions and normalised to the parent ion peak intensity. It is immediately clear that the obtained mass resolution is significantly lower for the ns-LIAD spectra. The primary cause for this was found to be an instability in the repeller electrode voltage, due to the nanosecond desorption laser pulse that hits this electrode in our current LIAD spectrometer design [16]. This effect was dependent on the incident desorption laser power, and at typical desorption laser fluences of 0.3 J/cm^2 reduced

the achievable resolution to around $\frac{M}{\Delta M} \sim 90$. This effect is completely absent in the case of cw-LIAD and a mass resolution of $\frac{M}{\Delta M} \sim 600$ was readily achieved.

For both desorption approaches the obtained spectrum is dominated by the parent ion peak at m/z 135. The higher resolution cw-LIAD spectrum shows no significant contribution from protonated or de-protonated adenine, which are commonly observed in sources containing hydrated adenine (i.e.adenine–water clusters) [23,24]. For the ns-LIAD case the reduced mass resolution means we cannot directly exclude contributions from (de)protonated adenine; however we see no further evidence for the generation of water clusters in the recorded spectra. Hence, our sample preparation and LIAD desorption, for both approaches, produced a high-density sample of intact adenine monomers.

The observed fragmentation pattern is very similar for both approaches, though with a slightly higher fragmentation rate observed for ns-LIAD. Since the ionisation laser pulses were identical in both approaches, this likely indicates a difference in internal temperature of the two samples, in turn leading to an enhanced fragmentation rate following ns-LIAD. Previous ns-LIAD studies have estimated sample temperatures of 500–700 K [16,25]. For the cw-LIAD no such measurements are available, but estimates of the foil surface temperature are in the range 350–400 K [26]. However, we do note that of course this depends on the exact experimental setup and parameters.

In order to assess the influence of the desorption laser on the produced molecular sample for ns-LIAD, we collected mass spectra at a range of desorption laser fluences (0.1 to 0.4 J/cm^2). The resulting yields of parent ion, as well as the fragments around masses 28-29 and 108, are shown in Fig. 2a as a function of desorption laser fluence. A steep increase in overall signal levels is observed (note the double logarithmic scale) for both parent and fragment ions. The observed parent signal is reasonably well described by a power-law relationship of the form $A \times x^n + b$, which yielded an exponent of $n = 5.1$. We also note that it was not feasible to increase the desorption laser fluence further, since this began to damage the titanium substrate.

Panel (b) in Fig. 2 shows the observed fragment-to-parent ratio for the two analysed mass ranges as a function of the desorption laser fluence. The relative fragmentation yield fluctuated due to the low signal levels, but overall appeared to be independent of the desorption laser fluence and constant within errors bars over the entire range investigated here. Hence, the desorption process does not seem to contribute to fragmentation of the adenine target molecule, in agreement with previous studies utilising femtosecond ionisation pulses [25]. The ns-LIAD technique is therefore a viable approach for the production of intact molecular target systems in the gas-phase, and for maximum target density should be operated at desorption laser intensities close to the damage threshold of the titanium foil. We also note that in our current LIAD setup the titanium foil is constantly replenished using a taper-design. At the employed foil speed of 125 µm/s this means that

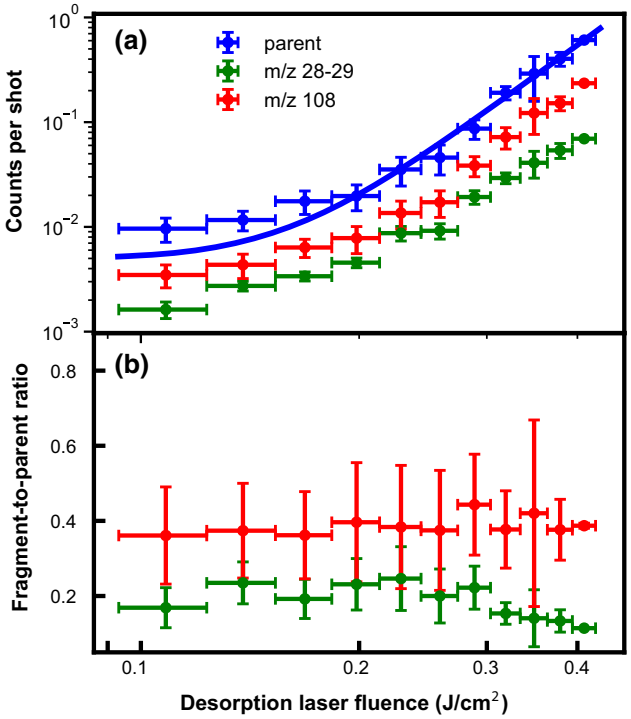

Fig. 2 Dependence of the ns-LIAD process on desorption laser fluence. **a** Ion yields for adenine parent and selected fragments at different desorption laser fluences, the solid line corresponds to a power-law fit (see text for details). **b** Observed fragment-to-parent ratios as a function of desorption fluence. All data was collected at $\sim 1.4 \times 10^{13}$ W/cm^2 ionisation intensity. Error bars show standard errors

subsequent laser shots from the 50 Hz desorption laser partially overlap on the foil, such that the maximum molecular plume density that can be achieved could be further increased by replenishing the foil faster.

We now turn to the cw-LIAD process. In order to assess the influence of the continuous desorption laser on the produced molecular sample, we again collected data at a range of desorption laser intensities (3–15 W/cm^2). This is shown in Fig. 3, for the parent ion, as well as the two selected fragments. Initially a very strong increase in signal was again observed for both parent and fragment ions, which however seemed to saturate at around 8 W/cm^2. Visual inspection of the foil substrate after the experiment showed that at the higher desorption intensities all sample appeared to be desorbed from the foil, explaining the observed saturation-type behaviour.

In Fig. 3b we show the associated fragment-to-parent ratios. At lower desorption laser intensities up to 4–5 W/cm^2 the ratio is very stable and constant, showing that also for cw-LIAD the desorption laser at these incident intensities does not lead to fragmentation of the target molecule, as has been previously found for other systems studied using the cw-LIAD approach [10]. Increasing the desorption intensity further, however, leads to a steep increase in the observed fragmentation. This clearly shows that when the incident intensity,

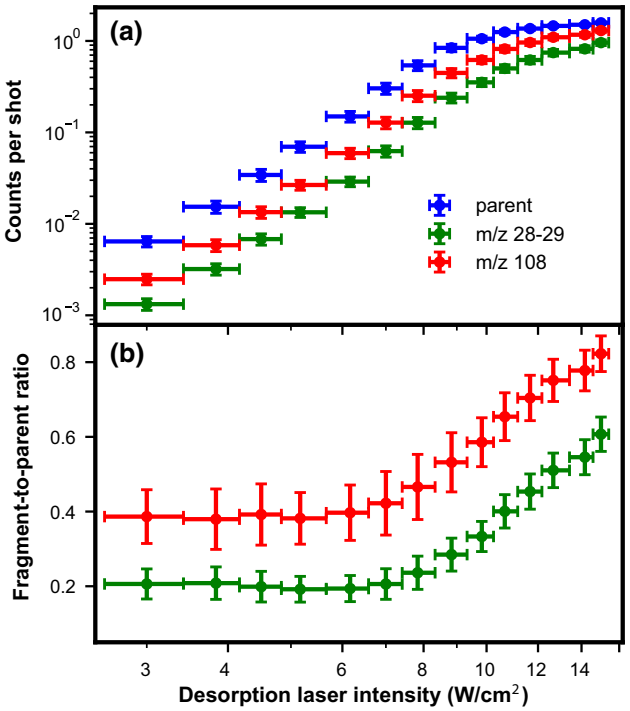

Fig. 3 Dependence of the cw-LIAD process on desorption laser intensity. **a** Ion yields for adenine parent and selected fragments at different desorption laser intensities. **b** Observed fragment-to-parent ratios as a function of desorption intensity. All data was collected at $\sim 1.4 \times 10^{13}$ W/cm^2 ionisation intensity. Error bars show standard errors

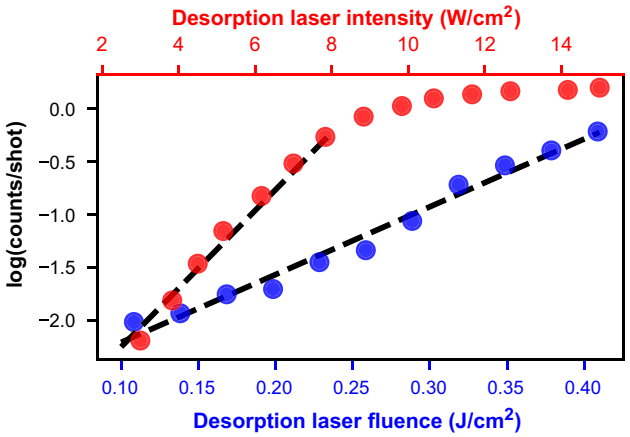

Fig. 4 Comparison of the observed parent ion signal as a function of desorption laser fluence for ns-LIAD (blue, bottom x-axis) or intensity for cw-LIAD (red, top x-axis). The dashed lines are the result of a linear fit to the data and highlight the region where the dependence can be described by a power-law

and hence the temperature of the foil substrate, is too high the target molecule can decompose before reaching the ionisation laser. The threshold for intact desorption of target molecules likely depends not only on the desorption setup used (laser wavelength, substrate material, heat dissipation), but also on the thermal properties of the target molecule itself. If one is careful to avoid excessive desorption powers, then the cw-LIAD approach appears to be a very attractive and continuous source of intact (bio) molecules. We also compared the absolute signal levels achieved for ns-LIAD and cw-LIAD under conditions where no additional fragmentation is observed, i.e. the highest fluence for ns-LIAD and around 5 W/cm^2 for cw-LIAD. This showed that the observed parent ion yield is around 2× higher for cw-LIAD.

The obtained results furthermore provide additional insight into the desorption mechanism at play during nanosecond pulsed or continuous LIAD. In Fig. 4 we directly compare the observed signal levels for the adenine parent ion as a function of incident desorption laser fluence (ns-LIAD, blue) or intensity (cw-LIAD, red). The y-axis is plotted here as the logarithm of the observed counts per shot to highlight the power-law behaviour as a function of desorption intensity, with the straight dashed lines showing a linear fit to the data. It is clear that for the ns-LIAD case the behaviour is well described by a power law across the entire desorption intensity range probed, as also shown in Fig. 2. The situation is very different for the cw-LIAD case. Here, the onset of a saturation of the signal is clearly observed at around 8 W/cm^2 of desorption intensity. At lower powers again a linear relationship is found. Notably the gradient of the desorption power dependence is very different for the two different desorption laser regimes, pointing at different underlying desorption processes.

In the case of cw-LIAD, it seems clear that desorption cannot be based on a mechanical or acoustic process, since the continuous laser does not induce any shock waves within the substrate. Desorption here must be due to a thermal process from a controlled and localised heating of the foil substrate, as has been previously discussed [10,26].

The situation is very different, however, in the case of ns-LIAD. The different dependence on the desorption laser already indicates that this is not a thermal process. Previous studies have furthermore observed that the velocity of molecules desorbed using ns-LIAD is independent of the desorption fluence, an observation which is also incompatible with a thermal desorption [16,17,25]. An alternative suggested mechanism for ns-LIAD is 'mechanical shake-off', the namesake of the LIAD technique, which proposes that the impulse of the nanosecond desorption laser leads to the formation of an acoustic wave travelling through the thin metal foil and mechanically desorbing molecules at the front. However, in our particular setup this mechanism can also be ruled out, since the formation of shock waves in metals typically requires significantly higher laser intensities [27], and should lead to desorption within fractions of a microsecond following laser irradiation [17], and not the tens of microsecond timescale observed in ns-LIAD studies [16].

Lastly, it has been suggested that the observed desorption might be due to the introduction of surface stress between the substrate and the sample layer, initiated by the nanosecond desorption pulse [17].

This mechanism, which is similar to mechanisms suggested for matrix-assisted laser desorption ionisation (MALDI) [28], assumes the presence of many isolated and independent 'sample islands' on the prepared foil substrate. The mechanical and/or thermal waves induced by the pulsed laser irradiation can then lead to surface stress between the islands of deposited sample and the metal substrate, and subsequently to elastic deformation and finally island decomposition and sample release. The internal energy of the desorbed molecules is hence only dependent on the binding energy between the sample and the substrate. This explains the independence of the molecular fragmentation on the incident desorption laser fluence observed here, as well as previous results showing that the velocity of desorbed molecules is independent of this also [16]. Our experiments thus add to the mounting evidence that for nanosecond pulsed LIAD sources, the desorption mechanism is dominated by surface-stress-induced desorption [15–17].This could be further corroborated by directly comparing different metal substrates under otherwise identical conditions.

4 Conclusion and outlook

We have presented the first direct comparison between nanosecond pulsed and continuous 'LIAD' sources, and evaluated the fragmentation behaviour of adenine during vaporisation. The use of a femtosecond multiphoton ionisation scheme enabled the analysis of the fragmentation due to the desorption process, and we found that both approaches can be operated in such a way that the desorption process does not induce analyte fragmentation. The data also yielded further insight into the desorption mechanisms behind LIAD. For the continuous case desorption must be due to a thermal process, and we found that applying excessive desorption power can lead to increased fragmentation. In the case of ns-LIAD a very different dependence on desorption power is observed, which is most compatible with a desorption mechanism dominated by stress-induced desorption from individual sample islands on the metal substrate. For both desorption regimes LIAD appears to be a powerful method to produce high density samples of intact biomolecules in the gas-phase, with numerous applications to gas-phase experiments that require pure samples, such as ultrafast dynamics or diffraction-based molecular imaging.

Acknowledgements This work was supported by the Netherlands Organization for Scientific Research (NWO) under grant numbers STU.019.009, 712.018.004 and VI-VIDI-193.037, and the European Regional Development Fund (EFRO Oost) under project 00949. We furthermore thank the Spectroscopy of Cold Molecules Department, and in particular Prof. Bas van de Meerakker, for continued support. For the permanent loan of the LIAD source we thank Prof. Jochen Küpper at DESY (Hamburg, Germany), a member of the Helmholtz Association HGF.

Author contributions

SW carried out the measurements with assistance from GLA and PK. SW and DAH analysed the data. AvR, MB and NJ constructed and implemented the experimental setup. DAH conceived the experiment and wrote the manuscript, with input from SW, GLA and PK.

Data Availability Statement This manuscript has no associated data or the data will not be deposited. [Authors' comment: The data that support the findings of this study are available upon reasonable request from the authors.]

Declarations

Conflict of interest The authors have no relevant financial or non-financial interests to disclose.

References

1. F.J. Vastola, A.J. Pirone, Ionization of organic solids by laser irradiation. Adv. Mass Spectrom. **4**, 107 (1968)
2. G. Meijer, M.S. de Vries, H.E. Hunziker, H.R. Wendt, Laser desorption jet-cooling of organic molecules - cooling characteristics and detection sensitivity. Appl. Phys. B **51**, 395–403 (1990). https://doi.org/10.1007/BF00329101
3. M.S. de Vries, P. Hobza, Gas-phase spectroscopy of biomolecular building blocks. Annu. Rev. Phys. Chem. **58**(1), 585–612 (2007). https://doi.org/10.1146/annurev.physchem.57.032905.104722
4. S.I. Ishiuchi, K. Yamada, H. Oba, H. Wako, M. Fujii, Gas phase ultraviolet and infrared spectroscopy on a partial peptide of β_2-adrenoceptor SIVSF-NH_2 by a laser desorption supersonic jet technique. Phys. Chem. Chem. Phys **18**, 23277–23284 (2016). https://doi.org/10.1039/C6CP04196E
5. J.M. Bakker, C. Plützer, I. Hünig, T. Häber, I. Compagnon, G. von Helden, G. Meijer, K. Kleinermanns, Folding structures of isolated peptides as revealed by gas-phase mid-infrared spectroscopy. Chem. Phys. Chem. **6**(1), 120–128 (2005). https://doi.org/10.1002/cphc.200400345

6. S. Bakels, M.P. Gaigeot, A.M. Rijs, Gas-phase infrared spectroscopy of neutral peptides: insights from the far-ir and thz domain. Chem. Rev. **120**(7), 3233–3260 (2020). https://doi.org/10.1021/acs.chemrev.9b00547
7. N. Teschmit, K. Długołecki, D. Gusa, I. Rubinsky, D.A. Horke, J. Küpper, Characterizing and optimizing a laser-desorption molecular beam source. J. Chem. Phys. **147**, 144204 (2017). https://doi.org/10.1063/1.4991639
8. B. Lindner, U. Seydel, Laser desorption mass spectrometry of nonvolatiles under shock wave conditions. Anal. Chem. **57**, 895–899 (1985). https://doi.org/10.1021/ac00281a027
9. C.R. Calvert, L. Belshaw, M.J. Duffy, O. Kelly, R.B. King, A.G. Smyth, T.J. Kelly, J.T. Costello, D.J. Timson, W.A. Bryan, T. Kierspel, P. Rice, I.C.E. Turcu, C.M. Cacho, E. Springate, I.D. Williams, J.B. Greenwood, LIAD-fs scheme for studies of ultrafast laser interactions with gas phase biomolecules. Phys. Chem. Chem. Phys. **14**(18), 6289–6297 (2012). https://doi.org/10.1039/c2cp23840c
10. J. Bocková, A. Rebelo, M. Ryszka, R. Pandey, D. Mészáros, P. Limão-Vieira, P. Papp, N.J. Mason, D. Townsend, K.L. Nixon, V. Vizcaino, J.C. Poully, S. Eden, Thermal desorption effects on fragment ion production from multi-photon ionized uridine and selected analogues. RCS Adv. **11**, 20612–20621 (2021). https://doi.org/10.1039/D1RA01873F
11. V.V. Golovlev, S.L. Allman, W.R. Garrett, N.I. Taranenko, C.H. Chen, Laser-induced acoustic desorption. Int. J. Mass Spectrom. Ion Process. **169–170**, 69–78 (1997). https://doi.org/10.1016/S0168-1176(97)00209-7
12. W.P. Peng, Y.C. Yang, M.W. Kang, Y.K. Tzeng, Z. Nie, H.C. Chang, W. Chang, C.H. Chen, Laser-induced acoustic desorption mass spectrometry of single bioparticles. Angew. Chem. Int. Ed. **45**, 1423–1426 (2006). https://doi.org/10.1002/anie.200503271
13. L. Nyadong, J.P. Quinn, C.S. Hsu, C.L. Hendrickson, R.P. Rodgers, A.G. Marshall, Atmospheric pressure laser-induced acoustic desorption chemical ionization mass spectrometry for analysis of saturated hydrocarbons. Anal. Chem. **84**(16), 7131–7137 (2012). https://doi.org/10.1021/ac301307p
14. R.C. Shea, C.J. Petzold, J.L. Campbell, S. Li, D.J. Aaserud, H.I. Kenttämaa, Characterization of laser-induced acoustic desorption coupled with a fourier transform ion cyclotron resonance mass spectrometer. Anal. Chem. **78**(17), 6133–6139 (2006). https://doi.org/10.1021/ac0602827
15. R.C. Shea, C.J. Petzold, J.a. Liu, H.I. Kenttämaa, Experimental investigations of the internal energy of molecules evaporated via laser-induced acoustic desorption into a fourier transform ion cyclotron resonance mass spectrometer. Anal. Chem. **79**(5), 1825–1832 (2007). https://doi.org/10.1021/ac061596x
16. Z. Huang, T. Ossenbrüggen, I. Rubinsky, M. Schust, D.A. Horke, J. Küpper, Development and characterization of a laser-induced acoustic desorption source. Anal. Chem. **90**(6), 3920–3927 (2018). https://doi.org/10.1021/acs.analchem.7b04797.1710.06684[physics]
17. A.V. Zinovev, I.V. Veryovkin, J.F. Moore, M.J. Pellin, Laser-driven acoustic desorption of organic molecules from back-irradiated solid foils. Anal. Chem. **79**(21), 8232–8241 (2007). https://doi.org/10.1021/ac070584o
18. F. Calegari, A. Trabattoni, A. Palacios, D. Ayuso, M.C. Castrovilli, J.B. Greenwood, P. Decleva, F. Martín, M. Nisoli, Charge migration induced by attosecond pulses in bio-relevant molecules. J. Phys. B: Atomic, Mol. Optical Phys. **49**(14), 142001 (2016). http://stacks.iop.org/0953-4075/49/i=14/a=142001
19. S.D. Camillis, J. Miles, G. Alexander, O. Ghafur, I.D. Williams, D. Townsend, J.B. Greenwood, Ultrafast nonradiative decay of gas-phase nucleosides. Phys. Chem. Chem. Phys. **17**(36), 23643–23650 (2015). https://doi.org/10.1039/C5CP03806E
20. U. Sezer, L. Wörner, J. Horak, L. Felix, J. Tüxen, C. Götz, A. Vaziri, M. Mayor, M. Arndt, Laser-induced acoustic desorption of natural and functionalized biochromophores. Anal. Chem. **87**(11), 5614–5619 (2015). https://doi.org/10.1021/acs.analchem.5b00601
21. D.J. Borton, L.M. Amundson, M.R. Hurt, A. Dow, J.T. Madden, G.J. Simpson, H.I. Kenttämaa, Development of a high-throughput laser-induced acoustic desorption probe and raster sampling for laser-induced acoustic desorption/atmospheric pressure chemical ionization. Anal. Chem. **85**(12), 5720–5726 (2013). https://doi.org/10.1021/ac4000333
22. G. Hass, A.P. Bradford, Optical properties and oxidation of evaporated titanium films*. J. Opt. Soc. Am. **47**(2), 125 (1957). https://doi.org/10.1364/JOSA.47.000125
23. N.J. Kim, Y.S. Kim, G. Jeong, T.K. Ahn, S.K. Kim, Hydration of DNA base cations in the gas phase. Int. J. Mass Spectrom. **219**(1), 11–21 (2002). https://doi.org/10.1016/S1387-3806(02)00547-X
24. B. Barc, M. Ryszka, J.C. Poully, E. Jabbour Al Maalouf, Z. el Otell, J. Tabet, R. Parajuli, P. van der Burgt, P. Limão-Vieira, P. Cahillane, M. Dampc, N. Mason, S. Eden, Multi-photon and electron impact ionisation studies of reactivity in adenine-water clusters. Int. J. Mass Spectrom. **365-366**, 194–199 (2014). https://doi.org/10.1016/j.ijms.2014.01.007
25. Z. Huang, D.A. Horke, J. Küpper. Laser-induced acoustic desorption of thermally stable and unstable biomolecules (2018). https://doi.org/10.48550/ARXIV.1811.05925
26. O. Ghafur, S.W. Crane, M. Ryszka, J. Bockova, A. Rebelo, L. Saalbach, S. De Camillis, J.B. Greenwood, S. Eden, D. Townsend, Ultraviolet relaxation dynamics in uracil: time-resolved photoion yield studies using a laser-based thermal desorption source. J. Chem. Phys. **149**(3), 034301 (2018). https://doi.org/10.1063/1.5034419
27. D..C. Swift, T..E. Tierney, R..A. Kopp, J..T. Gammel, Shock pressures induced in condensed matter by laser ablation. Phys. Rev. E **69**(3), 036,406 (2004). https://doi.org/10.1103/PhysRevE.69.036406
28. A. Vertes, R.D. Levine, Sublimation versus fragmentation in matrix-assisted laser desorption. Chem. Phys. Lett. **171**(4), 284–290 (1990). https://doi.org/10.1016/0009-2614(90)85365-J